Title: Experimental energy performance assessment of a solar desiccant cooling system in Southern Europe climates

Authors: F. Comino[1]*, J. Castillo González[2], F. J. Navas-Martos[2], M. Ruiz de Adana[1]

[1] Departamento de Química-Física y Termodinámica Aplicada, Escuela Politécnica Superior, Universidad de Córdoba, Campus de Rabanales, Antigua Carretera Nacional IV, km 396, 14071 Córdoba, España

[2] Centro Tecnológico del Plástico Andaltec, Polígono Industrial Cañada de la Fuente, Calle Vílches, s/n, 23600, Martos, Jaén, Spain

*Corresponding author tel. +34 626285994; e-mail: francisco.comino@uco.es (F. Comino)

Abstract

Solar desiccant cooling systems, SDEC, could be an effective alternative to conventional cooling systems, which mainly depend on electrical energy. The main objective of this work was to determine experimentally the seasonal coefficient of performance, SCOP, of a SDEC system composed of a desiccant wheel, an indirect evaporative cooler and a thermal solar system, to control indoor conditions in a research lab room. The dependence of coefficient of performance on outdoor air conditions and percentage of renewable energy used by the SDEC system were also analysed. Experimental tests were carried out for six weeks during spring and summer seasons in Martos, Spain.

The experimental results showed that the SDEC system independently adjusted the temperature and humidity of the supply air. 75% of the energy consumed by this air handling system comes from renewable sources. A seasonal coefficient of performance of the SDEC system of 2 was obtained for the period analysed. It is shown that the higher the outdoor temperature, the higher instantaneous COPs is. These results suggest that the use of SDEC systems in hot climates, such as southern European climates, could contribute to achieve the EU's energy goals within the frame of Nearly Zero Energy Buildings.

Nomenclature

c_p	specific heat [kJ kg^{-1} K^{-1}]
COP	instantaneous coefficient of performance [-]
DCOP	daily coefficient of performance [-]
E_{ren}	renewable energy used [%]
h	Enthalpy [kJ kg^{-1}]
P	pressure [Pa]
Q	thermal energy [kJ]
$\dot{Q}$	thermal power [kW]
RH	relative humidity [%]
SCOP	seasonal coefficient of performance [-]
t	time [s]
T	temperature [ºC]
$\dot{V}$	flow rate [m^3/h]
W	electric energy consumption [kJ]
$\dot{W}$	electric power [kW]

Greek letters

Δ	increment, decrement
ρ	density [kg m^{-3}]
ω	humidity ratio [g kg^{-1}]

Subscripts

a	air
c	cooling
d	dehumidification
DW	desiccant wheel
HC	heating coil
i	inlet
IEC	indirect evaporative cooler
L	latent
o	outlet
OA	outdoor air
S	sensible
T	total

Superscripts

$\bar{}$	average value

Acronyms

DW	desiccant wheel
EA	exhaust air
EC	evaporative cooler
F	fan
FT	filter
HC	heating coil
HE	heat exchanger
HP	hydraulic pump
HVAC	heating, ventilating and air conditioning
IEC	indirect evaporative cooler

NTC	negative temperature coefficient
OA	outdoor air
RA	return air
SA	supply air
SDEC	solar desiccant cooling
V	three-way valve

Keywords: hybrid HVAC system; solar desiccant cooling systems; energy efficiency; thermal solar system

1 Introduction

Nowadays, energy consumption in buildings in the EU is approximately 40% of the total energy consumption and 36% of the CO_2 emissions [1]. EU directives reinforced the goal of reducing energy consumption and the integration of renewable energies in buildings, instead of using fossil fuels [2]. A large part of current energy consumption and CO_2 emissions are due to heating, ventilating and air conditioning, HVAC, systems. Therefore, based on the European energy framework, the development of new efficient HVAC systems is required.

Currently, conventional HVAC systems based on vapour compression units are widely used. However, these systems present some restrictions due to the environmental problems derived from the use of refrigerant gases [3]. In addition, conventional HVAC systems suitably control air temperature, usually leaving the indoor moisture content in free evolution. Hybrid HVAC systems, composed of innovative elements, such as desiccant systems, evaporative cooling systems or renewable energy systems, could be an appropriate alternative to conventional air conditioning technologies. Hybrid HVAC systems could be very useful for combined control of indoor air temperature and humidity.

One type of air dehumidification system widely studied is the desiccant wheel, DW, [4–7]. Usually high regeneration air temperatures are demanded to carry out the desiccant dehumidification process, so a significant energy consumption is required to regenerate the DW. Renewable energy sources could be a safe and reliable solution to carry out the dehumidification

process and decarbonize the energy infrastructure. In addition, the main thermal demand of buildings, especially in the tertiary sector, such as offices or hotels, has a direct relationship with the hours of solar radiation that is received, where the thermal energy demand is increasing, in parallel to the available solar irradiance [8]. Several previous studies have analysed the thermal activation of a DW with a thermal solar system [9,10], achieving high energy savings in this process compared to conventional heating technologies, such as electric heaters or condensers of vapour compression units.

The heat generated by the dehumidification process of the DW causes the outlet process air temperatures to be high. Therefore, an efficient cooling system to reduce the high air temperatures generated in the dehumidification process and control the supply air temperature, would allow the sensible and latent heat to be decoupled. Numerous hybrid HVAC systems have been analysed by some authors in the available literature [11–14]. A DW integrated with a vapour compression system was analysed, where the evaporator was used to cool the process air and the condenser to thermally activate the DW [15,16], but these systems almost always depend on electrical energy. Other HVAC systems with a DW combined with an enthalpy wheel were widely studied [17–19]. These systems recover sensible heat from the process air flow in order to regenerate the wheel, achieving significant energy savings. Experimental studies of hybrid HVAC systems with a DW and a direct evaporative cooler, DEC, have previously performed [20]. However, DEC systems modify the supply air humidity ratio, so they do not allow the combined treatment of sensible and latent loads.

Recent research studies on desiccant cooling systems highlight that the combined use of a DW with an indirect evaporative cooler, IEC, is an effective alternative to conventional systems [21]. An IEC system is usually composed of a heat exchanger, HE, and an evaporative cooler, EC. Numerous hybrid HVAC systems composed of a desiccant liquid system and an IEC have been previously carried out [22,23]. However, not many studies have investigated the integration of a DW and an IEC. A parametric numerical study on a hybrid air conditioning system with a DW and an IEC designed for moderate climates obtained high energy efficiency values [24]. A

numerical study showed that a HVAC system composed of a DW and an IEC can adequately achieve indoor comfort conditions [25]. A numerical statistical study of a similar hybrid HVAC system was carried out, obtaining the most influential input variables on energy efficiency [26]. Other authors have also analysed numerically the thermal behaviour of hybrid HVAC systems composed of a DW and an IEC [27], obtaining significant energy savings for different climate zones compared to a conventional HVAC system based on direct expansion units. Numerical results of a desiccant cooling system combined with different collector types showed a reduction of primary energy consumption and of the equivalent CO_2 emissions of 50.2% and 49.8%, respectively, compared to a conventional system based in a chiller unit [28,29]. This latest hybrid HVAC configuration was also studied numerically for three DWs made of silica-gel, MILGO and zeolite-rich tuff, obtaining a primary energy saving of about 20%, 29%, 15%, respectively [30]. These authors also experimentally analysed a hybrid HVAC installation with a DW and a photovoltaic solar system located in Benevento (Italy), achieving significant reductions of CO_2, about 79%, respect to a conventional installation [31]. A daily experimental analysis of a HVAC system with a DW and IEC also showed a lower electrical energy consumption than that of a conventional HVAC system [32]. However, the use of hybrid DW IEC systems combined with solar thermal systems, using 100% outdoor air and controlling separately indoor conditions (air temperature and humidity) under South European climates requires detailed analysis of the energy performance.

The main objective of this work was to determine experimentally the seasonal energy performance of a solar desiccant cooling system, mainly composed of a DW, an IEC and a thermal solar system, to maintain indoor air conditions in a research lab room by controlling separately air temperature and humidity. Hence, seasonal experimental tests were carried out for six weeks of spring and summer in Martos (Jaén), Spain. The dependence of coefficient of performance on outdoor air conditions and percentage of renewable energy used by the SDEC system were analysed.

2 Material and methods

2.1 Solar desiccant cooling system

A solar desiccant cooling system, SDEC system, was installed to cool and dehumidify outdoor air for a research lab room. The process or supply air stream, states 1 to 3, the regeneration or exhaust air stream, states 4 to 6, and the secondary or exhaust air stream, states 7 to 9 are shown in Fig. 1.

The SDEC system was mainly composed of a DW to handle latent heat and a heat exchanger, HE, and an evaporative cooler, EC, to handle sensible heat. The combination of an HE and an EC is usually referred to as indirect evaporative cooling, IEC. The DW was activated by means of a heating coil, HC. The HC was fed by a constant water flow, which was heated by a thermal solar system. A small hydraulic pump was included to recirculate water in the EC. In addition, two air mixing boxes were integrated into the system in order to increase the desiccant and cooling capacity of the DW and the IEC system, respectively. Three centrifugal fans were selected to maintain the design air flow rate given the system pressure drop. A constant air flow rate of 1600 $m^3\ h^{-1}$ was considered for the three air streams. All the experimental tests were carried out using 100% outdoor air.

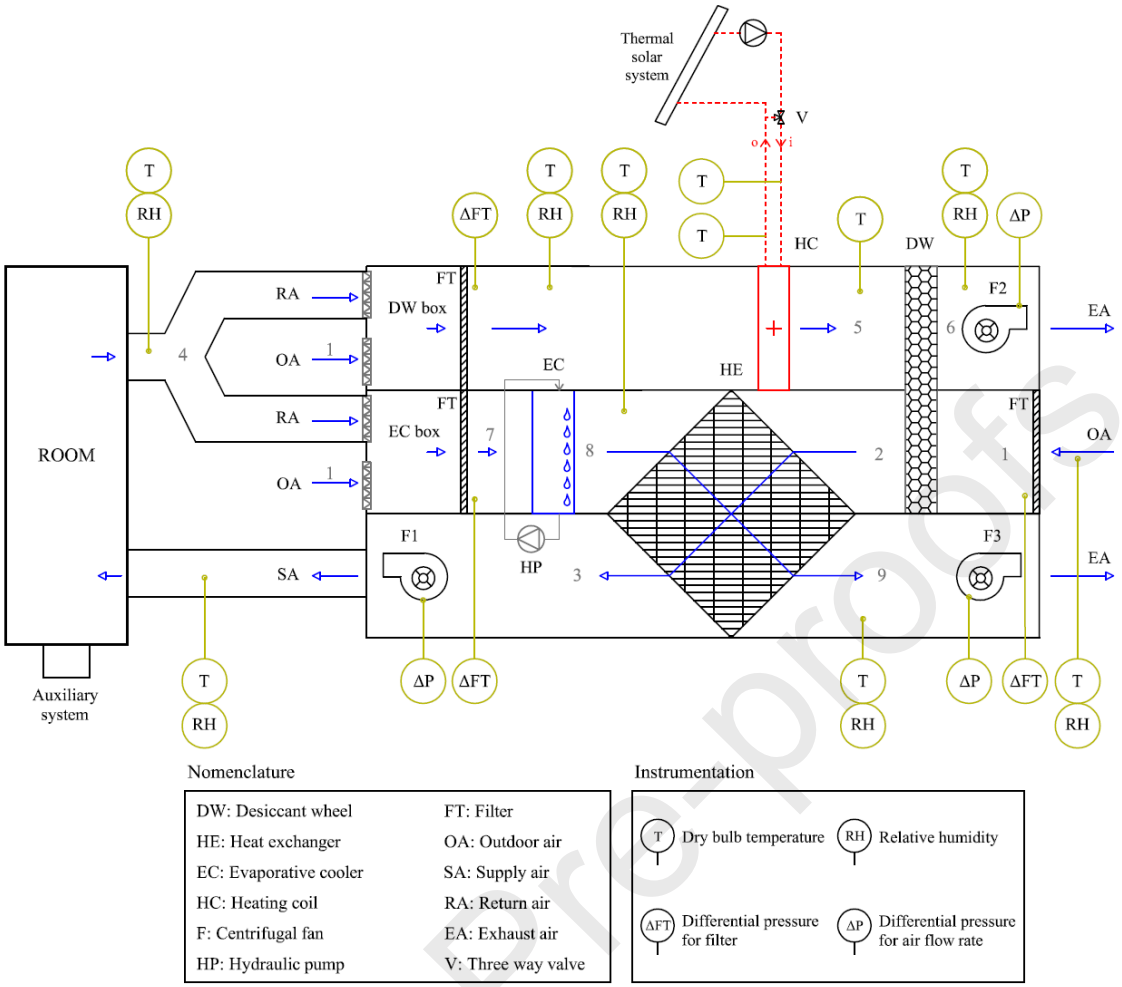

Fig. 1. Schematic of the experimental setup.

The technical characteristics of the HVAC equipment are shown in Table 1. It is noteworthy that, the HE plates were made of aluminium alloy and the DW was divided into two equal partitions and rotated at a constant speed of 15 rph. The matrix of the DW consisted of alternate layers of flat and corrugated sheets of silica gel and metal silicates, chemically bonded into a tissue of inorganic fibres. The centrifugal fans were designed to vary their electrical power in order to overcome the variable air pressure losses of the SDEC system components and thus ensure the set point air flow rates.

Table 1. Characteristics of the equipment.

Equipment	Value
Desiccant wheel (DW)	
Rotor size (diameter x thickness)	550 x100 mm
Nominal air flow rate	1600 m^3/h
Rotation speed	15 rph
Nominal desiccant capacity	10 kg/h
Desiccant material	Silica gel
Heat exchanger (HE)	
Air flow rate	1600 m^3/h
Plate material	Aluminium
Height	805 mm
Length	580 mm
Depth	805 mm
Evaporative cooler (EC)	
Sheet material	Fiberglass impregnated with additives
Height	600 mm
Length	600 mm
Total humidification	0,11 l/min
Pump nominal power	35 W
Pump Hmax	2.5 m
Water flow rate	500-2500 l/h
Heating coil (HC)	
Tube material	Smooth copper
Tube diameter	½''
Collectors	1''
Number of tubes	18
Finned length	600 mm
Rows of tubes	2
Fin passage	2,12 mm
Fans (F)	
Air flow rate	0 – 1600 m^3/h
Nominal power	400 W

The measured variables in the SDEC system, the type of sensor and its accuracy are summarized in Table 2. The locations of the sensors are shown in Fig. 1. The maximum values of standard deviations of the mean were ±0.5 ºC for the temperature, ±5 % for the relative humidity, ±5 Pa for the pressure difference to measure air flow rates, and ±6 % for the pressure difference to measure dirt in the filters The sampling time was 60 s throughout the day.

Table 2. Specification of measuring devices.

Measured parameter	Type	Accuracy
T	NTC (negative temperature coefficient)	± 0.5 ºC (T range 0 ºC to 50 ºC)
RH	Capacitive	± 5 % (RH range10% to 90%
ΔP	Differential pressure transmitter	±5 Pa (at range <500 Pa)
ΔFT	Differential pressure transmitter	± 6 % (50 Pa to 500 Pa)

2.2 Operation modes of the solar desiccant cooling system

The combination of HVAC elements of the SDEC system was designed to independently control the temperature and humidity of the room air. Hence, the SDEC system included a control system to adjust these HVAC elements. The control system checked the values the of indoor air temperature, T_4, indoor air humidity ratio, ω_4, and outdoor air temperature, T_1, at each time step, and then it executed the control actions, in order to reach the setpoint conditions. A diagram of the control logic of the SDEC system is represented in Fig. 2.

Three independent main control loops were considered in the SDEC system. The first one was an indoor air humidity control loop, the second one an indoor air temperature control loop and the third one an economizer loop.

The air humidity control loop was divided into two specific modes of operation, Mode 1-H and 2-H. This loop modulated the water flow rate of the regeneration heating coil, HC, and activated the rotation of the DW. The air temperature control loop was also divided into two specific modes of operation, Mode 1-T: when this reduction was required; and Mode 2-T: when there was no

need to reduce the air temperature. This loop only modulated the water flow rate of the hydraulic pump of the IEC. Finally, the economizer loop adjusted the position of the dampers in the DW and IEC boxes, in order to increase the desiccant and cooling capacity of the SDEC system. The return air stream, RA, passed through IEC air damper and the outdoor air stream, OA, passed through DW air damper when the outdoor air temperature was higher than the return air temperature, Mode 1-E. OA passed through IEC air damper and RA passed through DW air damper when the outdoor air temperature was lower than the return air temperature, Mode 2-E.

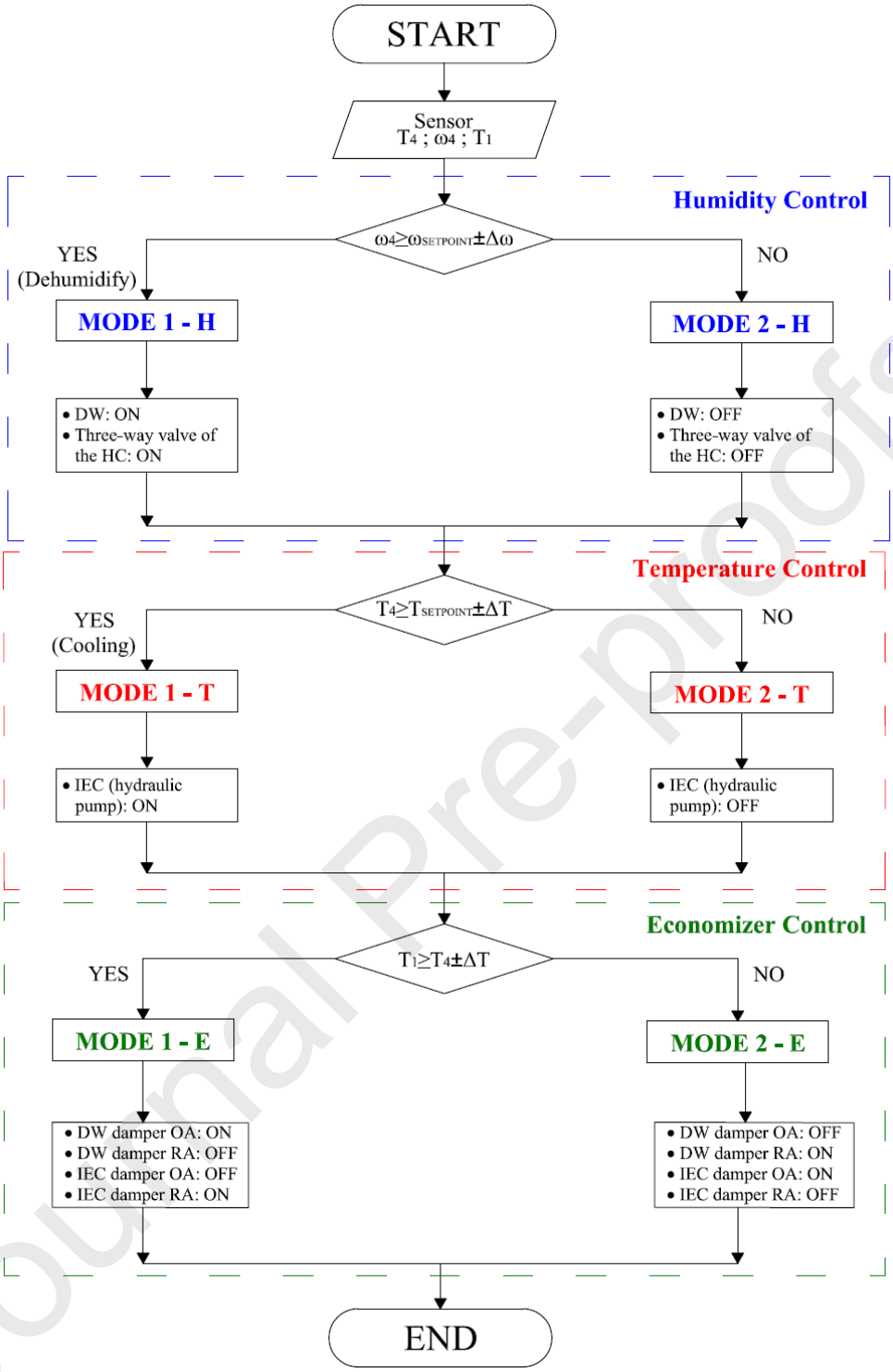

Fig. 2. SDEC system control logic diagram.

2.3 Thermal solar system

A thermal solar system of high efficiency vacuum tube collectors was designed, developed and manufactured in Plastic Technological Center (ANDALTEC), see Fig. 3. Each solar collector consisted mainly of one parabolic reflector and one solar collecting vacuum tube. The parabolic reflectors were manufactured by injection moulding in polycarbonate. The surfaces of the parabolic reflectors were covered with a thin aluminium film, in order to increase their reflection capacity. Direct flow vacuum tubes with flat absorbent surface were suitably assembled to the parabolic reflectors.

A collector module was composed of ten vacuum tubes and ten parabolic reflectors. Four collector modules composed the solar system, with an area of 3.69 m^2 each module on the horizontal axis. The angles of inclination of each collector module were the following: α= 80º (North-South inclination angle); θ= 10º (East-West angle of inclination).

The water heated by this system was used to feed the HC and thus thermally activate the DW by means of the regeneration air stream of the SDEC system, see Figure 1. The water flow rate that circulated through the solar system was 0.48 m^3/h.

Fig. 3. Image of the thermal solar system.

2.4 Research lab room

The SDEC system was designed to serve air in a research lab room of 63,8 m^3. The room was located in a building of the Plastic Technological Center (ANDALTEC) in Martos (Jaén), Spain. Four rotational terminal air units were installed in the room: two supply grilles terminal units and two exhaust grilles terminal units. Terminal units were connected with the SDEC system by means of air ducts. The characteristics of the room are summarized in Table 3.

In this work, the set point indoor conditions for the research lab room were set at 25±1 ºC for the air temperature and 8±1 g/kg for the air humidity ratio (40 % for the relative humidity).

Table 3. Characteristics of the research lab room.

Room	Floor area	28.3 m^2
	Height	2.3 m
	Exterior wall area (South and North)	8 m^2
	Exterior wall area (East and West)	18.9 m^2
	Exterior roof area	28.3 m^2
	Indoor air temperature	25 ºC
	Indoor relative humidity	40 %
U-value	Exterior wall	0.4 W m^{-2} K^{-1}
	Roof	0.32 W m^{-2} K^{-1}
Heat gain	Lighting	Sensible: 500 W
	People	7 persons
		Sensible: 64 W/person
		Latent: 81 W/person
	Research equipment	Sensible: 550 W
		Latent: 1173 W
Daily schedule	Monday-Friday: 08:00 am to 4:00 pm	

The room could demand cooling, dehumidification or both processes. This demand caused the SDEC system to deliver sensible thermal energy, latent thermal energy or both. Therefore, this system could work with three operating modes: (i) when the room demanded cooling and the SDEC system delivered sensible thermal energy, (ii) when the room demanded dehumidification and the SDEC system delivered latent thermal energy, or (iii) when the room demanded both processes and the SDEC system delivered sensible and latent thermal energy.

2.5 System performance

The SDEC system experimental tests were performed for six weeks of spring and summer, from May 27th to July 5th, 2019, in Martos (Jaén), Spain. The SDEC system performance was evaluated according to the following parameters. These parameters were calculated for three operating modes: (i) when the SDEC system delivered sensible thermal energy to cool the indoor air; (ii) when the SDEC system delivered latent thermal energy to dehumidify the indoor air; and (iii) when the SDEC system delivered sensible and latent thermal energy to cool and dehumidify the indoor air.

- Thermal energy delivered by the SDEC system to the supply air, Q. This parameter was calculated using an air flow energy balance for the three operating modes: sensible, latent and total energy delivered, $Q_{S,T}$, $Q_{L,T}$ and Q_T, respectively, expressed by Eqs. (1)-(3).

$$Q_{S,T} = \int_{t_{c,ON}}^{t_{c,OFF}} (\dot{Q}_{S,DW} + \dot{Q}_{S,IEC})\, dt \quad (1)$$

$$Q_{L,T} = \int_{t_{d,ON}}^{t_{d,OFF}} \dot{Q}_{L,DW}\, dt \quad (2)$$

$$Q_T = \int_{t_{c,d,ON}}^{t_{c,d,OFF}} (\dot{Q}_{S,T} + \dot{Q}_{L,T})\, dt \quad (3)$$

Each mode of operation caused the activation of different HVAC elements of the SDEC system, as shown in section 2.2, and consequently different electrical energy consumption, W.

- Electric energy consumption of the SDEC system was also obtained for the three operating modes: energy consumption when the SDEC system operated in sensible mode to cool the indoor air, $W_{S,}$ expressed by Eq. (4), in latent mode to dehumidify the indoor air, W_L, expressed by Eq. (5), and in sensible and latent mode to cool and dehumidify the indoor air during the entire period analysed, W_T, expressed by Eq. (6).

$$W_S = \int_{t_{c,ON}}^{t_{c,OFF}} (\dot{W}_{F1} + \dot{W}_{F2} + \dot{W}_{F3} + \dot{W}_{HP})\, dt \quad (4)$$

$$W_L = \int_{t_{d,ON}}^{t_{d,OFF}} (\dot{W}_{F1} + \dot{W}_{F2} + \dot{W}_{F3})\, dt \quad (5)$$

$$W_T = \int_{t_{c,d,ON}}^{t_{c,d,OFF}} (\dot{W}_{F1} + \dot{W}_{F2} + \dot{W}_{F3} + \dot{W}_{HP})\, dt \quad (6)$$

- Instantaneous coefficient of performance, COP, which measures the relation between the thermal power, $\dot{Q}$, and the electric power, $\dot{W}$. COP was obtained for the three operating modes: COP_S, COP_L, and COP_T, expressed by Eqs. (7)-(9).

$$COP_S = \frac{\dot{Q}_{S,T}}{\dot{W}_S} \quad (7)$$

$$COP_L = \frac{\dot{Q}_{L,T}}{\dot{W}_L} \quad (8)$$

$$COP_T = \frac{\dot{Q}_T}{\dot{W}_T} \quad (9)$$

- Daily coefficient of performance, DCOP, which measures the relation between the thermal energy delivered, Q, and the electric energy consumption, W, throughout the day. DCOP was also obtained for the three operating modes: $DCOP_S$, $DCOP_L$, and $DCOP_T$, expressed by Eqs. (10)-(12). Values of seasonal mean coefficient of performance, SCOP, was also calculated for the three operating modes. The SCOP vales were calculated using the same ratios of Eqs. (10)-(12), but for the entire period studied, six weeks.

$$DCOP_S = \frac{\int_{t_{c,ON}}^{t_{c,OFF}} \dot{Q}_{S,T}\, dt}{\int_{t_{c,ON}}^{t_{c,OFF}} \dot{W}_S\, dt} \quad (10)$$

$$DCOP_L = \frac{\int_{t_{d,ON}}^{t_{d,OFF}} \dot{Q}_{L,T}\, dt}{\int_{t_{d,ON}}^{t_{d,OFF}} \dot{W}_L\, dt} \quad (11)$$

$$DCOP_T = \frac{\int_{t_{c,d,ON}}^{t_{c,d,OFF}} \dot{Q}_T \, dt}{\int_{t_{c,d,ON}}^{t_{c,d,OFF}} \dot{W}_T \, dt} \quad (12)$$

Percentage of energy consumed by the overall experimental system from renewable energy sources to carry out the cooling and dehumidification processes, E_{ren}, was calculated for the entire period studied, Eq. (13). Where Q_{HC} is the thermal energy exchanged by the HC, calculated by Eq. (14), and $Q_{T,OA}$ is the total thermal energy delivered to the room from outside air, calculated by Eq. (15). $Q_{T,OA}$ was only calculated when the outside air helped to reach the set point conditions, that is, when the outdoor air temperature and humidity ratio were lower than the set point air temperature and humidity ratio.

$$E_{ren} = \frac{|Q_{HC}| + |Q_{T,OA}|}{|Q_{HC}| + |Q_{T,OA}| + |W_T|} \quad (13)$$

$$Q_{HC} = \int_{t_{d,ON}}^{t_{d,OFF}} \dot{V}_a \cdot \rho_a \cdot c_{p_a} \cdot (T_{a,i} - T_{a,o}) \, dt \quad (14)$$

$$Q_{T,OA} = \int_{t_{ON}}^{t_{OFF}} \dot{V}_a \cdot \rho_a \cdot (h_{a,setpoint} - h_{a,OA}) \, dt \quad (15)$$

3 Results

The energy analysis of the experimental results is presented in daily and seasonal analysis to correctly understand the behaviour of the SDEC system.

3.1 Daily behaviour of the solar desiccant cooling system

The thermal behaviour and energy consumption of the SDEC system for a typical hot day, May 27th, in Martos are represented in Fig. 4. Firstly, it can be observed than, at 8:00 AM, the return air humidity ratio, ω_4,was higher than the set point humidity ratio, fixed at 8 g/kg, see Fig. 4a. So, the dehumidification mode, Mode 1-H, was activated, see Fig. 4c, and the air streams were handled by the DW and the HC. The outdoor air stream was dehumidified and heated, from state

1 to state 2, see Fig. 4a and b. The return air temperature, T_4, was also higher than the set point air temperature, in the same period of time. Therefore, the Mode 1-T control activated the hydraulic pump of the IEC system, see Fig. 4c, reducing the supply air temperature, from T_2 to T_3, see Fig. 4b, and maintaining its constant air humidity ratio, ω_2 equal to ω_3, see Fig. 4a.

For this case study, the return air temperature, T_4, was higher than the outdoor air temperature, T_1, at the beginning of the period studied, so the return air, RA, passed through DW air damper and the outdoor air, OA, passed through IEC air damper, Mode 2-E, see Fig. 2 and state lines in Fig. 4c. The return air stream circulated by the HC and DW. Therefore, the return air temperature was raised by the HC and the thermal solar system, from T_4 to T_5, maintaining its constant air humidity ratio, ω_4 equal to ω_5. Then, the outlet air temperature of the HC was reduced and the air humidity ratio increased, from state 5 to state 6, see Fig. 4a and b. On the other hand, the outdoor air stream circulated by the EC and HE. The EC system reduced air temperature and increased air humidity ratio, from state 1 to state 8, see Fig. 4a and b. The HE exchanged sensible heat between state 8 and state 2. The return air temperature values were lower than the outdoor air temperature values at the end of the period studied, so the return air, RA, passed through IEC air damper and the outdoor air, OA, passed through DW air damper, Mode 1-E, see Fig. 4c.

The electric power, $\dot{W}$, values of the three centrifugal fans, F1, F2 and F3, and the hydraulic pump, HP, are shown in Fig. 4d. The highest $\dot{W}$ values were required by F2, mainly due to the HC and the regeneration side air pressure losses. It can be observed than the $\dot{W}$ values of F3 was significantly increased at 1:10 pm, due to the change in the opening of dampers and the new pressure losses generated, see Fig. 4c and d. The HP consumed electric energy only when the SDEC system required air cooling i.e. when the return air temperature satisfactorily did not achieve the set point air temperature, see Fig. 4d.

(a) Air humidity ratio

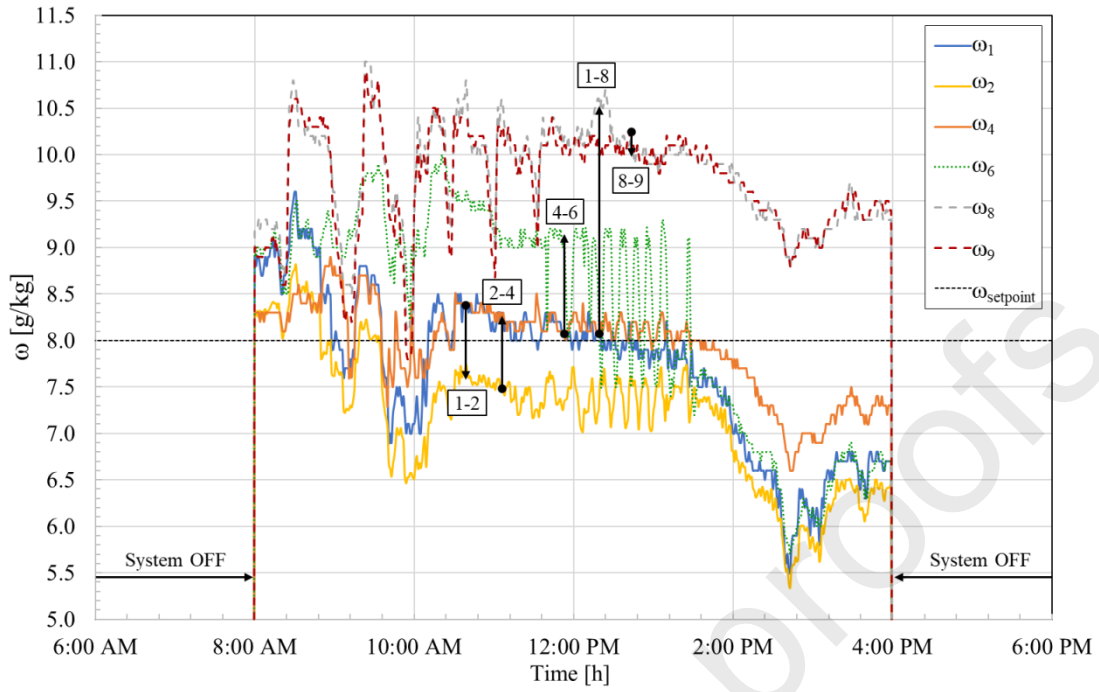

(b) Air temperature

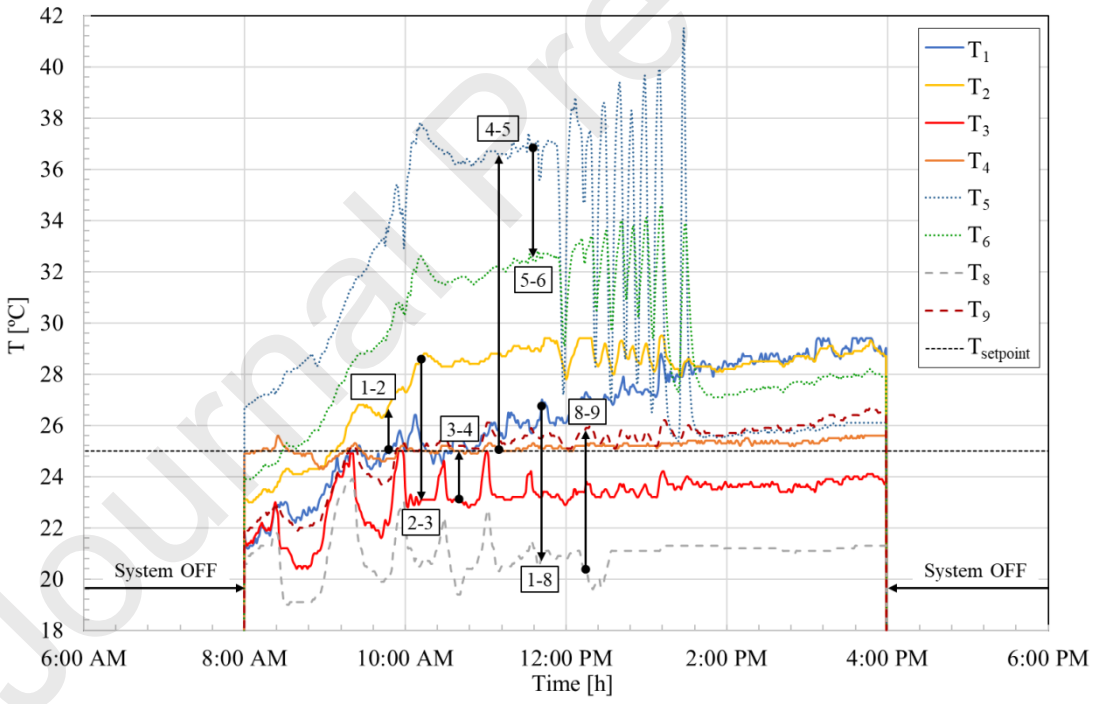

(c) States of the SDEC system

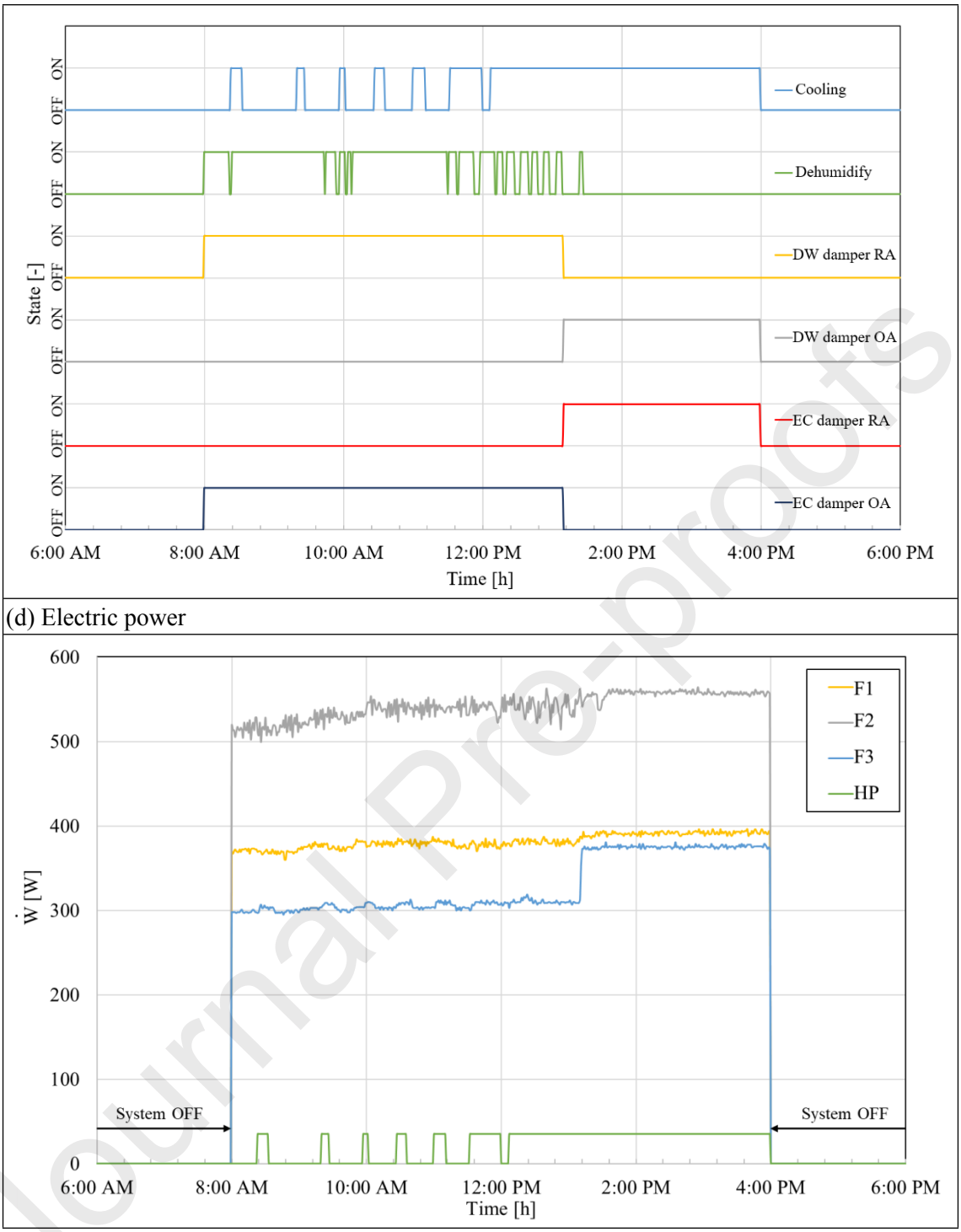

Fig. 4. Daily operational characteristics of the SDEC system.

3.2 Energy analysis

The sensible, latent and total thermal energy delivered by the SDEC system to the research lab room, the average daily outdoor air temperature, $\overline{T}_{OA}$, and average daily outdoor air humidity ratio, $\overline{\omega}_{OA}$, are represented in Fig. 5.

This figure shows sensible thermal energy delivered of the DW, the IEC and the entire solar desiccant cooling system, $Q_{S,DW}$, $Q_{S,IEC}$ and $Q_{S,T}$, respectively, latent thermal energy delivered of the DW and the entire system, $Q_{L,DW}$ and $Q_{L,T}$, respectively, whose values were the same because only the DW handled air humidity, and total thermal energy delivered of the entire system, Q_T. In this work, negative thermal energy delivered values were considered when the elements increased the air temperature and humidity ratio, while positive thermal energy delivered values were considered when the elements reduced the air temperature and humidity ratio. It can be observed that the DW delivered higher sensible and latent energy values, the higher the $\overline{\omega}_{OA}$ values, see Fig. 5a and b. The highest thermal energy delivered values of the DW were obtained on June 28th, -45.5 MJ and 25.3 MJ for $Q_{S,DW}$ and $Q_{L,DW}$, respectively, the day with the highest $\overline{\omega}_{OA}$ values, both with 11 g/kg. The $\overline{\omega}_{OA}$ values of some days were low, as for example on May 29th with 3.8 g/kg, see Fig. 5b. For these days, air dehumidification was not required, so the DW was not activated and it did not deliver sensible and latent energy.

The activation of the IEC was caused by three reasons:(i) sensible heat loads of the room; (ii) high values of outdoor air temperature, $\overline{T}_{OA}$; and (iii) sensible thermal energy delivered during the dehumidification process of the DW, $Q_{S,DW}$. Therefore, the highest $Q_{S,IEC}$ values were obtained for the days with the highest $\overline{T}_{OA}$values, such as on June 13th with 99.8 MJ for $\overline{T}_{OA}$ equal to 31 ºC, and the days with the highest $Q_{S,DW}$ values, such as on June 28th with 97.3 MJ for $Q_{S,DW}$ equal to -45.5 MJ, see Fig. 5a. The minimum $Q_{S,IEC}$ value was 12.7 MJ on May 30th, with an $\overline{T}_{OA}$value equal to 23 ºC, as shown in Fig. 5a. In this figure can also see that the $\overline{T}_{OA}$ values were similar on May 28th and June 1st, with 29.9 ºC and 29.7 ºC, respectively, however, the $Q_{S,IEC}$ values were

different, 97.3 MJ and 90.8 MJ, respectively. This sensible energy difference of the IEC was caused by the difference of $Q_{S,DW}$.

The values of total sensible and latent thermal energy delivered of the SDEC system, $Q_{S,T}$ and $Q_{L,T}$, respectively, the electric energy consumption when the cooling demand was required, W_S, and the energy consumption when the dehumidification demand was required, W_L, are also shown in see Fig. 5a and b by continuous lines. W_L was obtained from the electric energy consumption by the three centrifugal fans and W_S was obtained from the electric energy consumption by the three centrifugal fans and the hydraulic pump of the IEC. It can be observed that the W_S values were almost always lower than the $Q_{S,T}$ values. The W_S values followed trends similar to the $Q_{S,T}$ values, see Fig. 5a, mainly due to the operating time of the SDEC system. The maximum W_S value was 38 MJ on June 26th, with a $Q_{S,T}$ value equal to 60.5 MJ for this day, see Fig. 5a. The W_L values were similar to the W_S values when there was demand for air cooling and dehumidification, because the electric energy consumption of the hydraulic pump was low and the remaining electric energy consumption of the fans was the same. However, the W_L values were almost always higher than the $Q_{L,T}$ values. These results were mainly due to the fact that outdoor air conditions were favourable for the dehumidification of indoor air. Therefore, the need for air dehumidification was not high and the regeneration air temperature, T_5, was below 55 ºC. The maximum W_L value was 37 MJ on June 26th, with a $Q_{L,T}$ value equal to 20.7 MJ for this day, see Fig. 5b.

The values of total thermal energy delivered of the SDEC system, Q_T, and the total energy consumption, W_T, are shown in Fig. 5c. It can be observed that W_T was almost always lower than Q_T. The highest W_T values were found for the days with the highest Q_T, as shown in Fig. 5c.

(a) Sensible energy

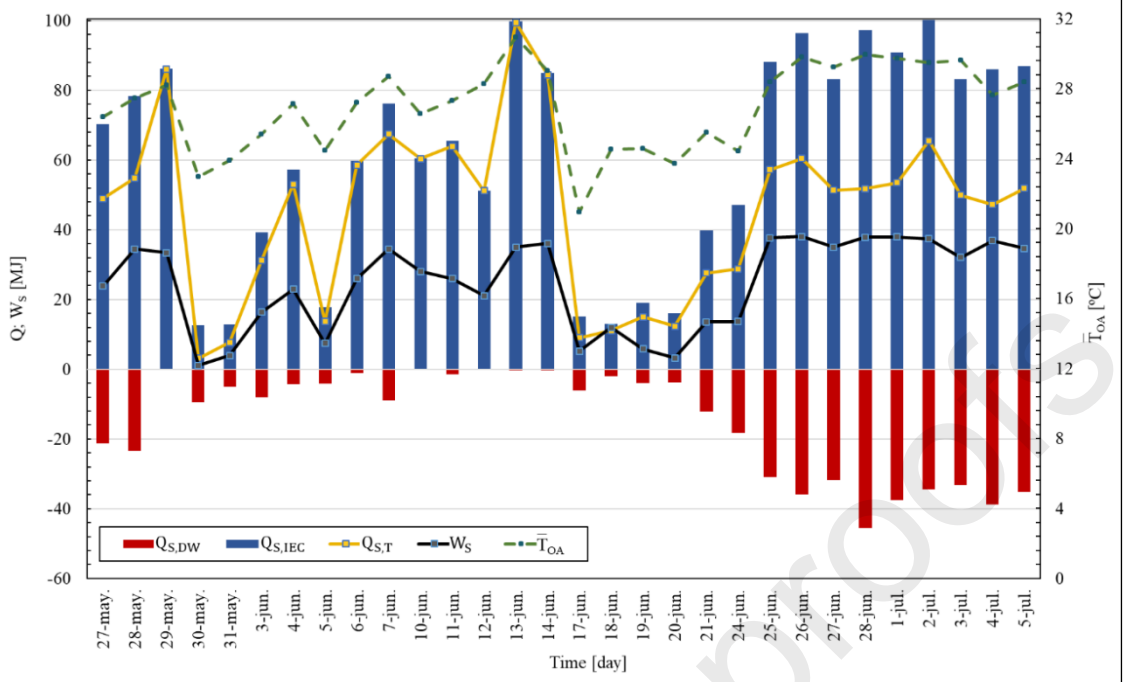

(b) Latent energy

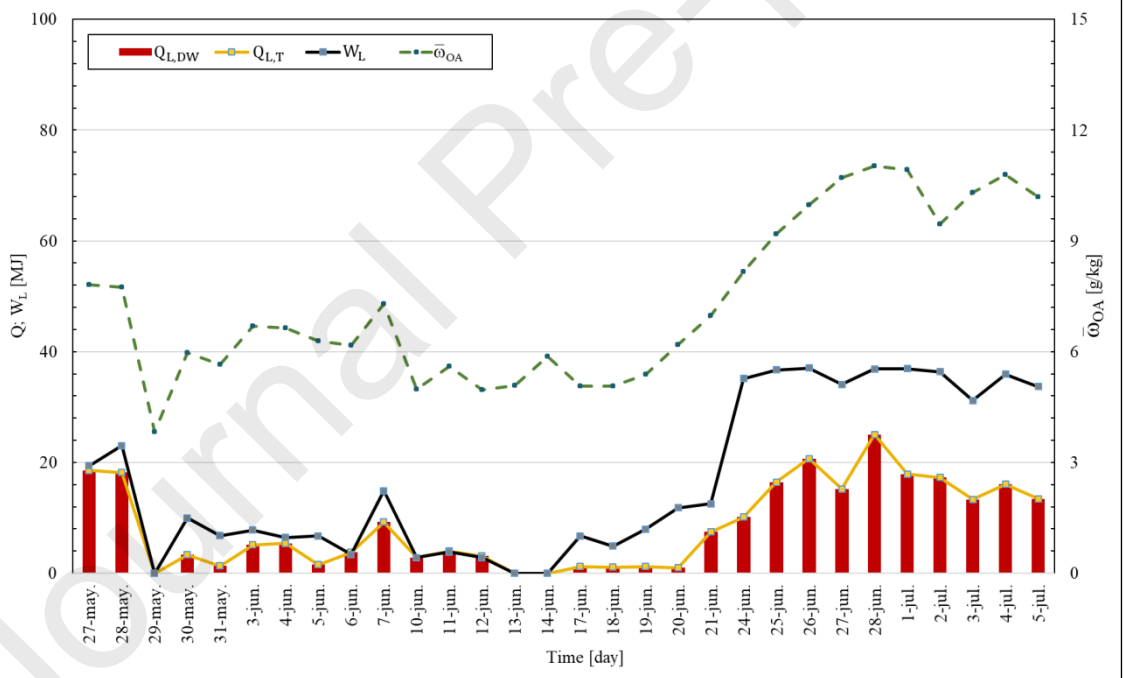

(c) Total energy

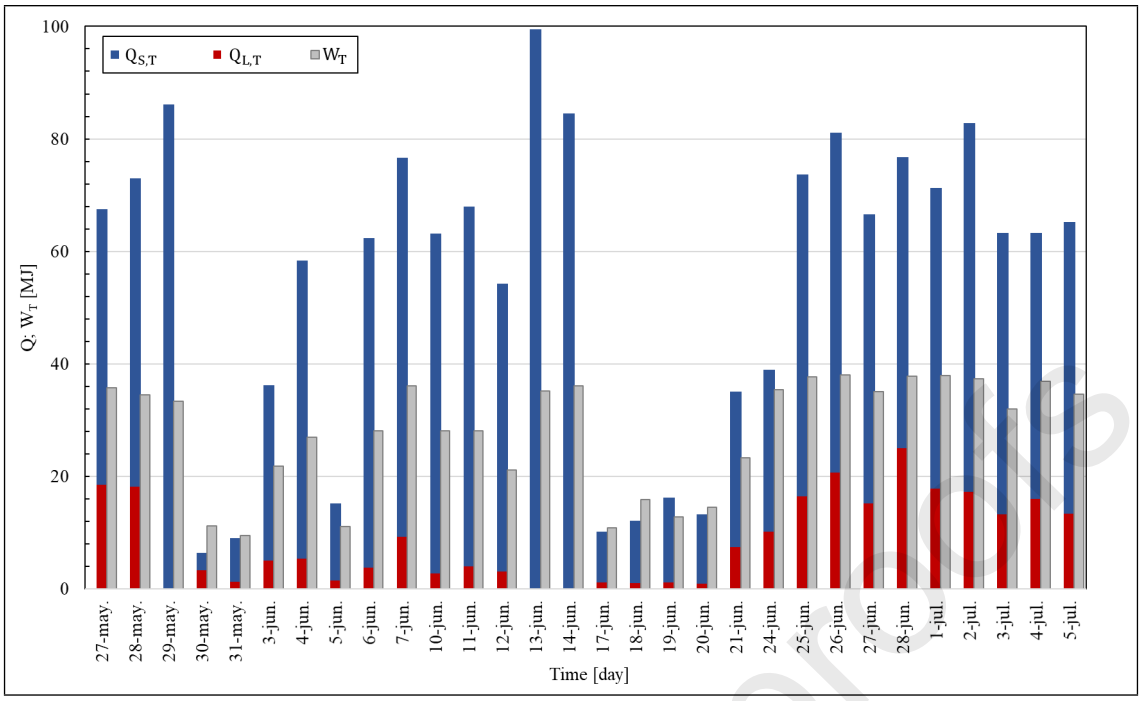

Fig. 5. Daily thermal energy delivered and electric energy consumption of the SDEC system.

3.2.1 Mean coefficient of performance

The values of daily mean coefficient of performance when the cooling demand was required, $DCOP_S$, when the dehumidification demand was required, $DCOP_L$, and when both processes were required, $DCOP_T$, are represented in Fig. 6. These results show the relationship between the thermal energy delivered and the electric energy consumption shown in Fig. 5. It can be observed that the $DCOP_S$ values were always greater than 1, less on June 18th, with a value equal to 0.9. The maximum $DCOP_S$ value was 3.8 on June 20th. However, the $DCOP_L$ values were almost always less than 1, because electric energy consumption of the SDEC system was higher than latent energy delivered. Some $DCOP_L$ values were equal to zero, because for these days there was not dehumidification demand, as shown in Fig. 5b. The maximum $DCOP_L$ value was 1.1 on June 6th and June 12th. Finally, the $DCOP_T$ values were also almost always greater than 1, with a maximum value of 2.8 on June 13th.

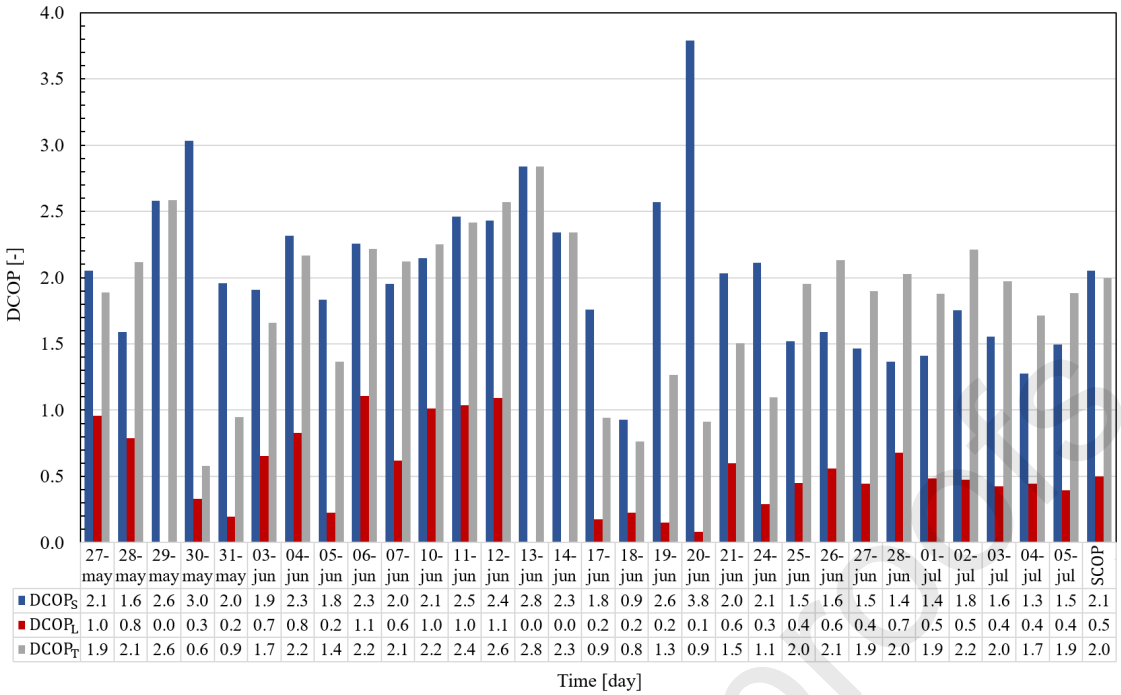

	27-may	28-may	29-may	30-may	31-may	03-jun	04-jun	05-jun	06-jun	07-jun	10-jun	11-jun	12-jun	13-jun	14-jun	17-jun	18-jun	19-jun	20-jun	21-jun	24-jun	25-jun	26-jun	27-jun	28-jun	01-jul	02-jul	03-jul	04-jul	05-jul	SCOP
$DCOP_S$	2.1	1.6	2.6	3.0	2.0	1.9	2.3	1.8	2.3	2.0	2.1	2.5	2.4	2.8	2.3	1.8	0.9	2.6	3.8	2.0	2.1	1.5	1.6	1.5	1.4	1.4	1.8	1.6	1.3	1.5	2.1
$DCOP_L$	1.0	0.8	0.0	0.3	0.2	0.7	0.8	0.2	1.1	0.6	1.0	1.0	1.1	0.0	0.0	0.2	0.2	0.2	0.1	0.6	0.3	0.4	0.6	0.4	0.7	0.5	0.5	0.4	0.4	0.4	0.5
$DCOP_T$	1.9	2.1	2.6	0.6	0.9	1.7	2.2	1.4	2.2	2.1	2.2	2.4	2.6	2.8	2.3	0.9	0.8	1.3	0.9	1.5	1.1	2.0	2.1	1.9	2.0	1.9	2.2	2.0	1.7	1.9	2.0

Fig. 6. Daily mean coefficient of performance of the SDEC system.

3.2.2 Renewable energy used

The percentages of daily renewable energy used by the SDEC system are shown in Fig. 7. It can be observed than significant percentages were used, always over 60 %, see Fig. 7. The maximum percentage of daily renewable energy used was 85.5 % on June 24th. The remaining percentages came from electrical energy.

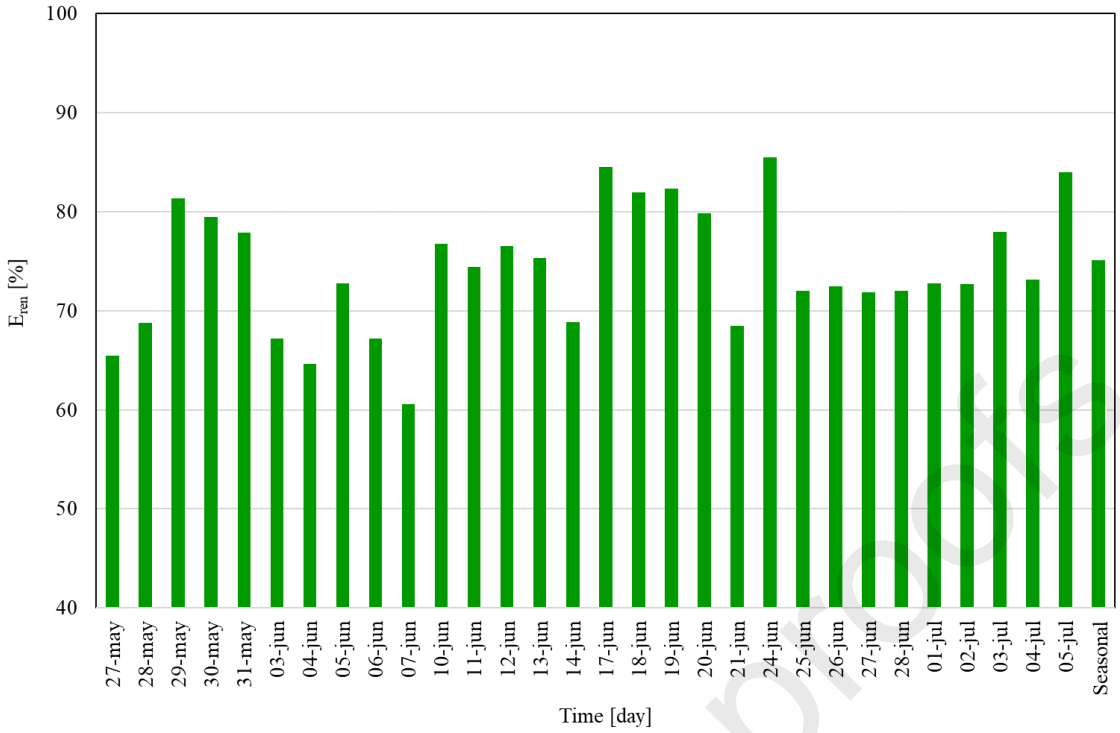

Fig. 7. Renewable energy used by the SDEC system.

3.2.3 Auxiliary energy

The SDEC system allowed to cool and dehumidify air with high percentages of renewable energy. However, sometimes the SDEC system did not achieve the set point conditions. So, auxiliary energy was required to achieve the set point conditions. Two typical examples, June 20th and 25th, are shown in Fig. 8. During both days cooling and dehumidification demand was required. On June 20th, it can be observed that the SDEC system did not require auxiliary sensible and latent energy, Fig. 8a, the set point conditions were achieved throughout the day. On June 25th, the results shows that auxiliary latent energy was required when solar heat gain was low, especially before 12:00 AM, and the outdoor air humidity ratio values were over the humidity ratio set point of 8 g/kg, as shown Fig. 8b. $\dot{Q}_{L,aux}$ decreased when solar heat gain increased along with time. The maximum $\dot{Q}_{L,aux}$ value was 2.3 kW at 8:00 AM. A thermal storage system could reduce the auxiliary latent energy required by the SDEC system. Auxiliary sensible energy was also required for high outdoor air temperature values, values higher than 30 ºC, see Fig. 8b. The maximum

$\dot{Q}_{S,aux}$ value was 0.9 kW at 4:00 PM. These results suggest that an energy optimization of the IEC system could reduce auxiliary sensible energy required and increase its energy efficiency. The current average energy efficiency of the evaporative cooler system was 0.6, so this system could be further improved.

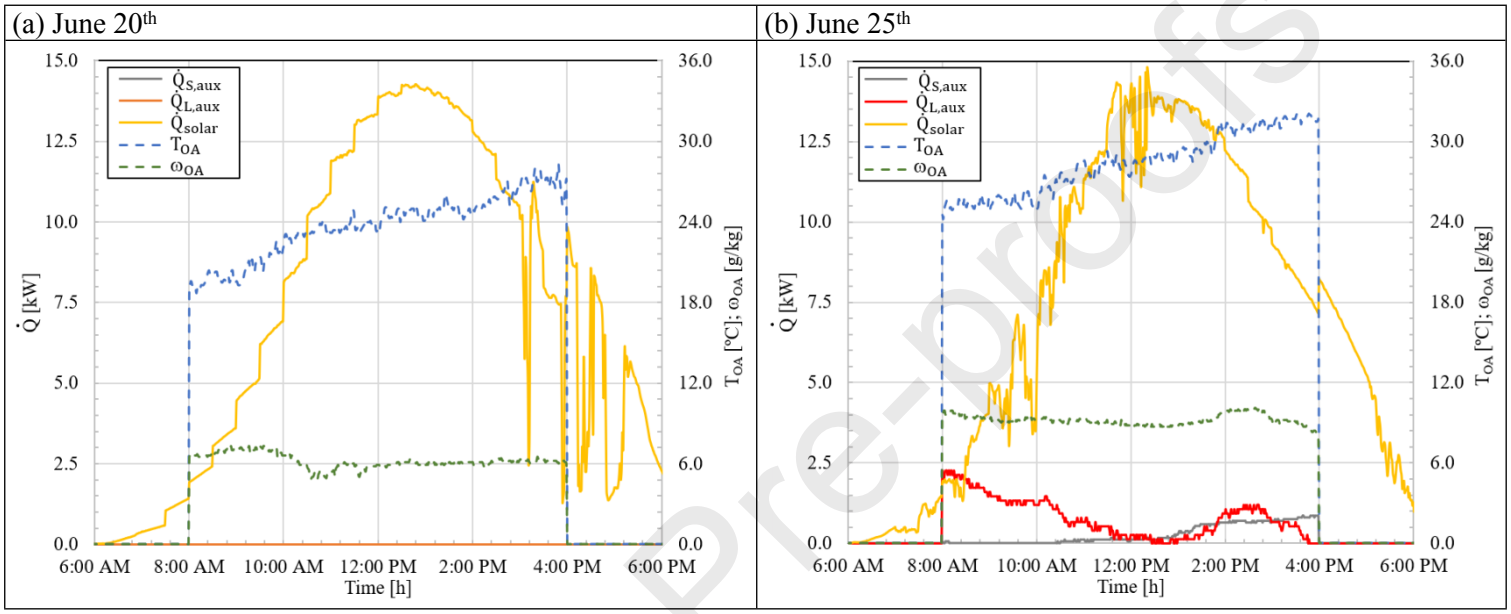

Fig. 8. Auxiliary energy required of the SDEC system.

3.3 Overall energy analysis

The results of daily mean coefficient of performance when the cooling demand was required, $DCOP_S$, showed variations between 0.9 and 3.8, see Fig. 6. In this section, instantaneous COP_S values were calculated for each measured time step, 60 s, for the entire period studied. The dependence of the outdoor air temperature on the COPs values is represented in Fig. 9. These values were divided according to two specific modes of operation: (i) Mode 1-E when T_{OA} was higher than T_{RA}, so the return air stream, RA, passed through IEC; (ii) and Mode 2-E when T_{OA} was lower than T_{RA}, so the outdoor air stream, OA, passed through IEC, see Fig. 2.

The dependence of the outdoor air temperature on the COPs values shows a positive linear trend, that is, when the outdoor air temperature values increased, the COP_S values also increased, as

shown Fig. 9. An inverse trend to this is usually obtained with air cooling systems based on direct expansion units, which reduce their COP_S values when outdoor air temperature increased. In this figure, it can also be observed the lowest COP_S values were obtained when the outdoor air stream, OA, passed through IEC. This mode of operation occurred when T_{OA} was lower than T_{RA}, so low cooling demand was required. Nevertheless, the highest COP_S values were obtained when the return air stream, RA, passed through IEC, T_{OA} was higher than T_{RA} and high cooling demand was required. It is shown that the higher T_{OA} values, the higher COP_S values. These results suggest that the energy performance of the SDEC system increase for hot climate zones.

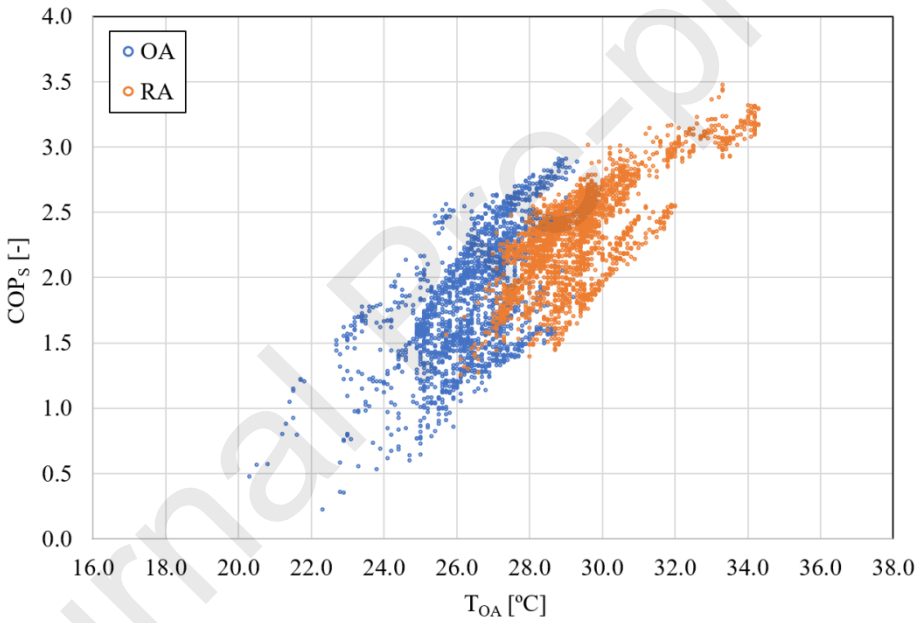

Fig. 9. Outdoor air temperature on instantaneous sensible coefficient of performance when the cooling demand was required.

The average instantaneous energy performance values, $\overline{COP}$, and the seasonal energy performance values, SCOP, of the SDEC system for the entire period studied are summarized in Table 4. It can be observed that the values of $\overline{COP}_L$ and $SCOP_L$ were the same, 0.5. Nevertheless, the values of $SCOP_S$ and $SCOP_T$, 2.1 and 2, respectively, improved seasonally compared to the instantaneous values of $\overline{COP}_S$ and $\overline{COP}_T$, 1.8 and 1.7, respectively, as shown in Table 4. These SCOP values were

also represented in Fig. 6. This $SCOP_T$ value shows good agreement with the $SCOP_T$ values, between 2 and 2.8, obtained from several numerical simulations of a similar desiccant cooling system, mainly composed of a DW and an IEC, carried out in previous works [27]. Other recent experimental studies on solar desiccant cooling systems obtained a $SCOP_T$ value lower than that obtained in the present work, $SCOP_T$ equal to 0.91 without including the electric energy consumption [9]. A significant percentage of seasonal renewable energy was used by the SDEC system to handle air of the research lab room, 75.1%, see Table 4.

Table 4. Overall results of the SDEC system.

Parameters	Value
$\overline{COP_S}$	1.8
$\overline{COP_L}$	0.5
$\overline{COP_T}$	1.7
$SCOP_S$	2.1
$SCOP_L$	0.5
$SCOP_T$	2.0
E_{ren}	75.1 %

4 Conclusions

In this study, a solar desiccant cooling system, SDEC system, mainly composed of a DW, an IEC and a thermal solar system, was analysed experimentally to maintain indoor air conditions in a research lab room located in Martos (Jaen), Spain. The thermal energy delivered by the SDEC system, the seasonal coefficient of performance, SCOP, and the percentage of renewable energy, E_{ren}, were studied for six weeks during spring and summer seasons under climatic conditions in southern Europe. The following conclusions were obtained from the present work:

- The experimental configuration and the control system allowed the SDEC system to independently control the sensible and latent loads of the room using 100% outdoor air.

A low percentage of auxiliary energy is required to maintain indoor conditions in the period analysed.

- The sensible thermal energy delivered by the SDEC system in cooling mode was higher than its electric energy consumption. Hence a sensible seasonal coefficient of performance, $SCOP_S$, value of 2.1 was obtained. On the contrary, a 0.5 value of seasonal latent coefficient of performance, $SCOPL_L$, was found in dehumidification mode for the same period. This is mainly due to the dehumidification potential of outdoor air. A value of 2 was found for the total seasonal coefficient of performance, $SCOP_T$, when the SDEC was operated in cooling and dehumidification mode for the entire period analysed.
- It is noteworthy that, 75% of the seasonal energy consumed by the SDEC system to carry out the cooling and dehumidification processes came from renewable sources, such us thermal solar energy and outdoor air.
- It was found a significant dependence of the sensible coefficient of performance of the SDEC system with outdoor air temperature. For the analysed period, the higher the outdoor air temperature, the higher the sensible coefficient of performance, COP_S, is.

It can be concluded that the analysed SDEC system maintains indoor conditions by using 100% outdoor air and handling independently air temperature and humidity in hot climate areas. Moreover, an important percentage of the SDEC system energy consumption came from renewable energy sources, like solar thermal systems.

These results suggest that solar desiccant cooling systems, SDEC, could be considered as an alternative to traditional direct expansion systems. Therefore, the use of SDEC systems in hot climates, such as South European climates, could contribute to achieve the EU's energy goals within the frame of Nearly Zero Energy Buildings.

Acknowledgements

The authors acknowledge the financial support received from European Union's Horizon 2020 research and innovation programme under grant agreement Nº857801 through the Project with reference H2020-WIDESPREAD2018-03-857801, entitled WEDISTRICT-Smart and local reneWable Energy DISTRICT heating and cooling solutions for sustainable living.

References

[1] European Commission, www.ec.europa.eu, (2015).

[2] European Parliament, European Directive 2010/31/EU on the Energy Performance of Buildings, 2010. doi:doi:10.3000/17252555.L_2010.153.eng.

[3] European Commission, Regulation (EU) No 517/2014 of the European Parliament and of the Council of 16 April 2014 on fluorinated greenhouse gases and repealing Regulation (EC) No 842/2006, Off. J. Eur. Union. (2014). doi:https://doi.org/10.4271/1999-01-0874.

[4] F. Comino, M. Ruiz de Adana, F. Peci, First and second order simplified models for the performance evaluation of low temperature activated desiccant wheels, Energy Build. 116 (2016) 574–582. doi:10.1016/j.enbuild.2016.02.005.

[5] F. Comino, M. Ruiz de Adana, Experimental and numerical analysis of desiccant wheels activated at low temperatures, Energy Build. 133 (2016). doi:10.1016/j.enbuild.2016.10.021.

[6] S. De Antonellis, M. Intini, C.M. Joppolo, L. Molinaroli, F. Romano, Desiccant wheels for air humidification: An experimental and numerical analysis, Energy Convers. Manag. 106 (2015) 355–364. doi:10.1016/j.enconman.2015.09.034.

[7] G. Angrisani, F. Minichiello, C. Roselli, M. Sasso, Experimental analysis on the dehumidification and thermal performance of a desiccant wheel, Appl. Energy. 92 (2012) 563–572. doi:10.1016/j.apenergy.2011.11.071.

[8] C. Infante Ferreira, D.S. Kim, Techno-economic review of solar cooling technologies based on location-specific data, Int. J. Refrig. 39 (2014) 23–37. doi:10.1016/j.ijrefrig.2013.09.033.

[9] G. Qadar Chaudhary, M. Ali, N.A. Sheikh, S.I. ul H. Gilani, S. Khushnood, Integration of solar assisted solid desiccant cooling system with efficient evaporative cooling technique for separate load handling, Appl. Therm. Eng. 140 (2018) 696–706. doi:10.1016/j.applthermaleng.2018.05.081.

[10] K.F. Fong, T.T. Chow, C.K. Lee, Z. Lin, L.S. Chan, Comparative study of different solar cooling systems for buildings in subtropical city, Sol. Energy. 84 (2010) 227–244. doi:10.1016/j.solener.2009.11.002.

[11] D.B. Jani, M. Mishra, P.K. Sahoo, Application of artificial neural network for predicting performance of solid desiccant cooling systems – A review, Renew. Sustain. Energy Rev. 80 (2017) 352–366. doi:10.1016/j.rser.2017.05.169.

[12] J. Guo, S. Lin, J.I. Bilbao, S.D. White, A.B. Sproul, A review of photovoltaic thermal (PV/T) heat utilisation with low temperature desiccant cooling and dehumidification, Renew. Sustain. Energy Rev. 67 (2017) 1–14. doi:10.1016/j.rser.2016.08.056.

[13] D.B. Jani, M. Mishra, P. Kumar, A critical review on application of solar energy as renewable regeneration heat source in solid desiccant – vapor compression hybrid cooling system, J. Build. Eng. 18 (2018) 107–124. doi:10.1016/j.jobe.2018.03.012.

[14] G. Angrisani, C. Roselli, M. Sasso, F. Tariello, G. Vanoli, Performance Assessment of a Solar-Assisted Desiccant-Based Air Handling Unit Considering Different Scenarios, Energies. 9 (2016) 724. doi:10.3390/en9090724.

[15] Y. Sheng, Y. Zhang, Y. Sun, L. Fang, J. Nie, L. Ma, Experimental analysis and regression prediction of desiccant wheel behavior in high temperature heat pump and desiccant wheel air-conditioning system, Energy Build. 80 (2014) 358–365.

doi:10.1016/j.enbuild.2014.05.040.

[16] D.B. Jani, M. Mishra, P.K. Sahoo, Experimental investigation on solid desiccant-vapor compression hybrid air-conditioning system in hot and humid weather, Appl. Therm. Eng. 104 (2016) 556–564. doi:10.1016/j.applthermaleng.2016.05.104.

[17] C.R. Ruivo, F. Fernández Hernández, J.M. Cejudo López, Influence of the desiccant wheel effectiveness method approaches, with fix and variable effectiveness parameters, on the performance results of an airport air-conditioning system, Energy Convers. Manag. 94 (2015) 458–471. doi:10.1016/j.enconman.2015.01.090.

[18] M. El Hourani, K. Ghali, N. Ghaddar, Effective desiccant dehumidification system with two-stage evaporative cooling for hot and humid climates, Energy Build. 68 (2014) 329–338. doi:10.1016/j.enbuild.2013.09.040.

[19] W.M. El-Maghlany, A.A. ElHefni, M. ElHelw, A. Attia, Novel air conditioning system configuration combining sensible and desiccant enthalpy wheels, Appl. Therm. Eng. 127 (2017) 1–15. doi:10.1016/j.applthermaleng.2017.08.020.

[20] A.M. Baniyounes, M.G. Rasul, M.M.K. Khan, Experimental assessment of a solar desiccant cooling system for an institutional building in subtropical Queensland, Australia, Energy Build. 62 (2013) 78–86. doi:10.1016/j.enbuild.2013.02.062.

[21] F. Comino, S. Milani, S. De Antonellis, C.M. Joppolo, M. Ruiz de Adana, Simplified performance correlation of an indirect evaporative cooling system: development and validation, Int. J. Refrig. 88 (2018) 307–317. doi:10.1016/j.ijrefrig.2018.02.002.

[22] W.Z. Gao, Y.P. Cheng, A.G. Jiang, T. Liu, K. Anderson, Experimental investigation on integrated liquid desiccant e Indirect evaporative air cooling system utilizing the Maisotesenko e Cycle, Appl. Therm. Eng. 88 (2015) 288–296. doi:10.1016/j.applthermaleng.2014.08.066.

[23] H.J. Kim, S.J. Lee, S.H. Cho, J.W. Jeong, Energy benefit of a dedicated outdoor air system

over a desiccant-enhanced evaporative air conditioner, Appl. Therm. Eng. 108 (2016) 804–815. doi:10.1016/j.applthermaleng.2016.07.185.

[24] D. Pandelidis, A. Pacak, A. Cichoń, S. Anisimov, P. Drąg, B. Vager, V. Vasilijev, Multi-stage desiccant cooling system for moderate climate, Energy Convers. Manag. 177 (2018) 77–90. doi:10.1016/j.enconman.2018.09.061.

[25] D. Pandelidis, S. Anisimov, W.M. Worek, P. Drag, Comparison of desiccant air conditioning systems with different indirect evaporative air coolers, Energy Convers. Manag. 117 (2016) 375–392. doi:10.1016/j.enconman.2016.02.085.

[26] J.D. Chung, D.Y. Lee, Contributions of system components and operating conditions to the performance of desiccant cooling systems, Int. J. Refrig. 34 (2011) 922–927. doi:10.1016/j.ijrefrig.2011.03.003.

[27] F. Comino, M. Ruiz de Adana, F. Peci, Energy saving potential of a hybrid HVAC system with a desiccant wheel activated at low temperatures and an indirect evaporative cooler in handling air in buildings with high latent loads, Appl. Therm. Eng. 131 (2018). doi:10.1016/j.applthermaleng.2017.12.004.

[28] G. Angrisani, C. Roselli, M. Sasso, F. Tariello, Assessment of Energy, Environmental and Economic Performance of a Solar Desiccant Cooling System with Different Collector Types, Energies. (2014) 6741–6764. doi:10.3390/en7106741.

[29] F. Calise, M. Dentice, C. Roselli, M. Sasso, F. Tariello, Desiccant-based AHU interacting with a CPVT collector: Simulation of energy and environmental performance, Sol. Energy. 103 (2014) 574–594. doi:10.1016/j.solener.2013.11.001.

[30] P. Bareschino, F. Pepe, C. Roselli, M. Sasso, F. Tariello, Desiccant-Based Air Handling Unit Alternatively Equipped with Three Hygroscopic Materials and Driven by Solar Energy, (2019).

[31] C. Roselli, M. Sasso, F. Tariello, Assessment of a solar PV-driven desiccant-based air

handling unit with different tracking systems, Sustain. Energy Technol. Assessments. 34 (2019) 146–156. doi:10.1016/j.seta.2019.04.013.

[32] P. Finocchiaro, M. Beccali, B. Nocke, Advanced solar assisted desiccant and evaporative cooling system equipped with wet heat exchangers, Sol. Energy. 86 (2012) 608–618. doi:10.1016/j.solener.2011.11.003.

SUPPLEMENTARY MATERIAL

Psychrometric analysis of the SDEC system for typical operation modes

The behaviour of the SDEC system for two case studies on May 27th, see Fig. 4, is represented in Fig. 10 by psychrometric charts. Air states 1-4 correspond to the air processes shown in Fig. 1. The first case, Fig. 10a, represents the behaviour of the SDEC system at 3 PM, where the modes of operation Mode 2-H and Mode 1-T were activated, see Fig. 2. For this case, the process air temperature was reduced 3.8 ºC, from T_1 to state T_3, however, ω_1 was lower than the setpoint humidity ratio, 8 g/kg, so air dehumidification was not required. The second case study, Fig. 10b, represents the behaviour of the SDEC system at 12:10 PM, where the modes of operation Mode 1-H and Mode 1-T were activated, see Fig. 2. Air dehumidification and cooling was required for these outdoor air conditions, with reductions of 1.8 g/kg and 1.9 ºC, respectively, from state 1 to state 3. In Fig. 10, it can also be observed the experimental uncertainty of measurements, see Table 2. The air temperature deviation was always constant, ±0.5 ºC, however, the air humidity ratio deviation was slightly higher for high air temperatures, with maximum value of ±1 g/kg.

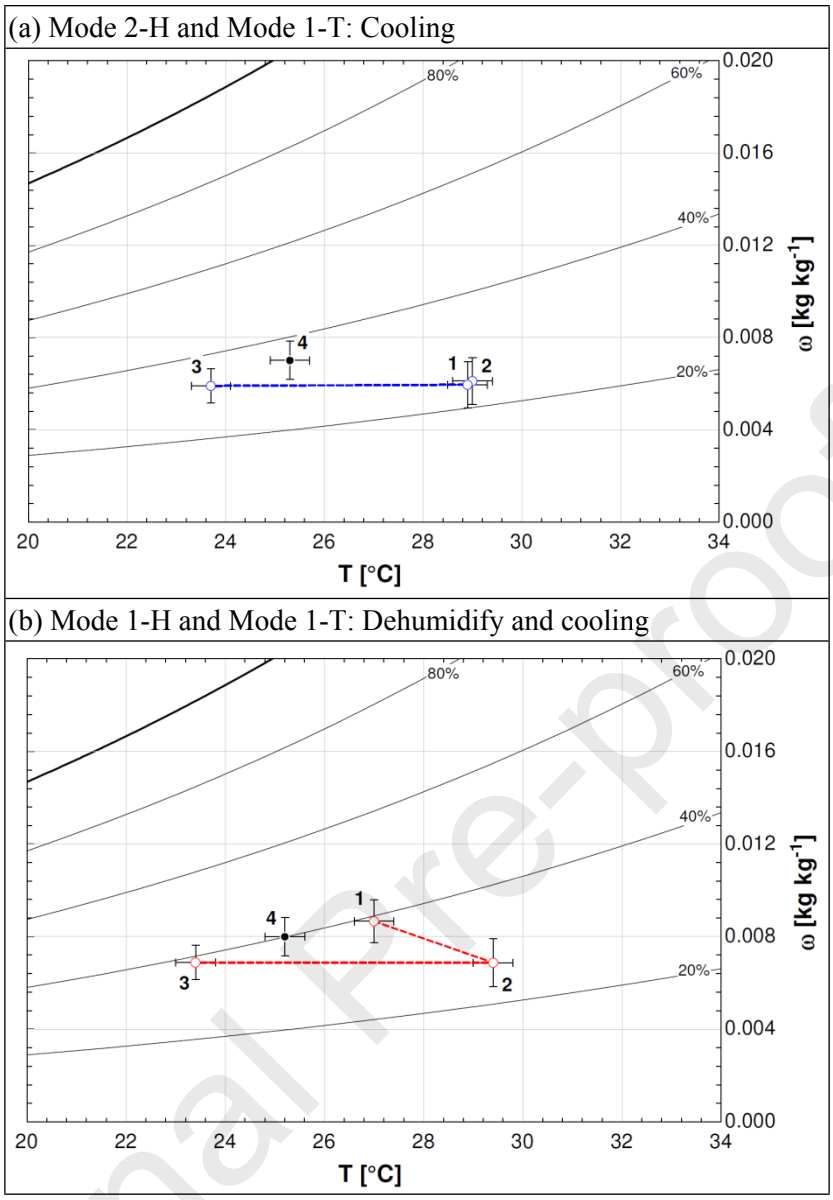

Fig. 10. Process air conditions and room air conditions of the SDEC system for two case studies.

Experimental energy performance assessment of a solar desiccant cooling system in Southern Europe climates

Highlights:

- Seasonal energy performance of a solar desiccant cooling system was analysed.
- This system used significant percentages of renewable energy, always over 60 %.
- High values of seasonal coefficient of performance were found.